Role for Plasma Membrane–Related Ca^{2+}-ATPase-1 (ATP2C1) in Pancreatic β-Cell Ca^{2+} Homeostasis Revealed by RNA Silencing

Kathryn J. Mitchell, Takashi Tsuboi, and Guy A. Rutter

Changes in intracellular Ca^{2+} concentration play a key role in the regulation of insulin secretion by glucose and other secretagogues. Here, we explore the importance of the secretory pathway Ca^{2+}-ATPase, plasma membrane–related Ca^{2+}-ATPase-1 (PMR1; human orthologue ATP2C1) in intracellular Ca^{2+} homeostasis in pancreatic islet β-cells. Endogenous PMR1 mRNA and protein were detected in both isolated rat islets and β-cell–derived lines (MIN6 and INS1). Subcellular fractionation of the cell lines revealed PMR1 immunoreactivity in both microsomal and dense-core secretory vesicle–enriched fractions. Correspondingly, depletion of cellular PMR1 with small interfering RNAs inhibited Ca^{2+} uptake into the endoplasmic reticulum and secretory vesicles by ~20%, as assessed using organelle-targeted aequorins in permeabilized INS1 cells. In intact cells, PMR1 depletion markedly enhanced flux though L-type Ca^{2+} channels and augmented glucose-stimulated, but not basal, insulin secretion. Whereas average cytosolic $[Ca^{2+}]$ increases in response to 30.0 mmol/l glucose were unaffected by PMR1 depletion, $[Ca^{2+}]$ oscillation shape, duration, and decay rate in response to glucose plus tetraethylammonium were modified in PMR1-depleted single cells, imaged using fluo-3-acetoxymethylester. PMR1 thus plays an important role, which is at least partially nonoverlapping with that of sarco(endo-) plasmic reticulum Ca^{2+}-ATPases, in the control of β-cell Ca^{2+} homeostasis and insulin secretion. *Diabetes* 53: 393–400, 2004

Glucose-stimulated insulin secretion involves the closure of ATP-sensitive K^+ channels (1) and influx of Ca^{2+} through voltage-gated Ca^{2+} channels (2). However, intracellular Ca^{2+} stores are also implicated in the control by glucose of β-cell $[Ca^{2+}]$ oscillations and electrical activity (3) and in the response to potentiators of secretion such as acetylcholine (4,5). Although these stores are thought largely to correspond to the endoplasmic reticulum (ER) and Golgi complex in β-cells (6), we recently provided evidence for a role for dense-core secretory vesicles in β-cell Ca^{2+} homeostasis (7–9). Moreover, whereas sarco(endo-)plasmic reticulum Ca^{2+}-ATPases (SERCAs), members of the P-type Ca^{2+}-transporting ATPase family (10), play an important role in the accumulation of Ca^{2+} by the ER, the identity of the Ca^{2+}-ATPases involved in Ca^{2+} sequestration into other stores, including dense-core secretory vesicles, is less clear.

Plasma membrane–related Ca^{2+}-ATPase-1 (PMR1; human nomenclature ATP2C1), a member of the secretory pathway Ca^{2+}-ATPase family (11,12), is a Ca^{2+}- and Mn^{2+}-transporting ATPase (13) localized to the Golgi, or a Golgi subcompartment, in budding yeast (14), where it appears to be of importance for the normal functioning of the secretory pathway. Thus, *Saccharomyces cerevisiae* mutants lacking functional PMR1 exhibit defects in protein glycosylation, processing, and sorting (14). More recent studies examining the role of overexpressed *Caenorhabditis elegans* PMR1 in mammalian cell lines have demonstrated its targeting to a thapsigargin-insensitive Ca^{2+} store, with functional properties that differ from those of the ER and that are of importance in generating and modifying cellular Ca^{2+} signals (15). Moreover, genetic studies on human patients have revealed that mutations in ATP2C1 lead to Hailey-Hailey disease, an autosomal dominant skin disorder characterized by persistent blisters and erosions of the skin (16,17). PMR1 is also implicated in the control of Ca^{2+} entry in both yeast and mammalian cell systems. Thus, Ca^{2+} entry is stimulated in *S. cerevisiae* PMR1–null mutants (18,19) by a mechanism involving activation of a high-affinity Ca^{2+} influx system, likely to be a voltage-gated Ca^{2+} channel (19). Additionally, after Ca^{2+} reintroduction to Ca^{2+}-depleted mammalian COS-1 cells overexpressing PMR1, the free cytosolic Ca^{2+} concentration ($[Ca^{2+}]_{cyt}$) increased after a latency period, indicating a mechanism involving regenerative Ca^{2+} release (20).

From the Henry Wellcome Laboratories of Integrated Cell Signaling and Department of Biochemistry, School of Medical Sciences, University Walk, University of Bristol, Bristol, U.K.

Address correspondence and reprint requests to Guy A. Rutter, Henry Wellcome Laboratories of Integrated Cell Signaling and Department of Biochemistry, School of Medical Sciences, University Walk, University of Bristol, Bristol, BS8 1TD, U.K. E-mail: g.a.rutter@bris.ac.uk.

Received for publication 21 July 2003 and accepted in revised form 22 October 2003.

Additional information for this article can be found in an online appendix at http://diabetes.diabetesjournals.org.

$[Ca^{2+}]_{cyt}$, free cytosolic Ca^{2+} concentration; ER, endoplasmic reticulum; FBS, fetal bovine serum; fluo-3-AM, fluo-3-acetoxymethylester; HRP, horseradish peroxidase; KRBB, Krebs-Ringer bicarbonate buffer; m6PR, mannose-6-phosphate receptor; PMR1, plasma membrane–related Ca^{2+}-ATPase-1; PMSF, phenylmethylsulfonyl fluoride; RyR II, type II ryanodine receptor; SERCA, sarco(endo-)plasmic reticulum Ca^{2+}-ATPase; siRNA, small interfering RNA; TEA, tetraethylammonium; VAMP, vesicle-associated membrane protein.

Here, we extend the list of physiological processes in which this novel Ca^{2+}-ATPase appears to play an important role to include pancreatic β-cell Ca^{2+} homeostasis, using RNA silencing (21–24) to reduce the expression of endogenous PMR1 in these cells. We combine this novel methodology with Ca^{2+} imaging techniques involving recombinant targeted probes to dynamically monitor [Ca^{2+}] changes selectively within individual intracellular organelles. These approaches reveal that the mammalian homologue of PMR1 plays an important role in controlling Ca^{2+} entry into β-cells and usually acts as a suppressor of insulin secretion.

RESEARCH DESIGN AND METHODS

Cell culture, transfection, and adenoviral infection. Rat β-cell–derived INS1 cells (25) were cultured in RPMI-1640 medium (Gibco BRL) containing 11 mmol/l glucose and 2 mmol/l glutamine, supplemented with 10% (vol/vol) fetal bovine serum (FBS), 100 units/ml penicillin, 100 μg/ml streptomycin, 1 mmol/l sodium pyruvate, and 50 μmol/l β-mercaptoethanol. Mouse β-cell–derived MIN6 cells (26) were cultured in Dulbecco's modified Eagle's medium (Sigma) containing 25 mmol/l glucose and 2 mmol/l pyruvate, supplemented with 15% (vol/vol) FBS, 4 mmol/l glutamine, 100 units/ml penicillin, 100 μg/ml streptomycin, and 50 μmol/l β-mercaptoethanol. For [Ca^{2+}] measurements with recombinant targeted aequorins (see below), cells were seeded onto 13-mm diameter poly-L-lysine–coated glass coverslips and grown to 50–80% confluency. Cells were then infected with adenoviruses encoding untargeted cytosolic aequorin (Cyt.Aq) (27) or aequorin targeted to either the secretory vesicle matrix by fusion with vesicle-associated membrane protein-2 (VAMP2)/synaptobrevin (VAMP.Aq) (7) or the ER lumen (ER.Aq) (28), at a multiplicity of infection of 30 infectious units per cell. Measurements of aequorin bioluminescence were performed 48 h after infection using a purpose-built photomultiplier system, as described previously (7,29). Rat islets were isolated and cultured as described (30).

Detection of PMR1 mRNA in pancreatic β-cells and islets. Total RNA was extracted from cell lines or rat tissue using TRI reagent (Sigma) according to the manufacturers' instructions and then reverse-transcribed using M-MLV reverse transcriptase (Promega). PCR amplification was performed with primers designed to amplify a 640-bp fragment of PMR1 corresponding to nucleotides 327–967 of RAT PMR1 mRNA (31): forward, 5′-GTTAGTCATAGGCGAGC-3′; reverse, 5′-GTCCATGCTCTTCTGCAG-3′. The full coding region of mouse PMR1 and a portion of the 3′ untranslated region (nucleotides 179-3016) (31) was amplified from MIN6 cells by PCR: forward primer, 5′-ATGAAGGTTGCACGATTTC-3′; reverse primer, 5′-CCTCTTGAACTTGCCCTTC-3′.

Preparation of cell lysates and membrane fractions. Rat islets (~150) or clonal β-cells were extracted into radioimmunoprecipitation assay buffer, comprising PBS supplemented with 1% (vol/vol) Nonidet P40, 0.5% (wt/vol) sodium deoxycholate, 0.1% (wt/vol) SDS, 1 μmol/l phenylmethylsulfonyl fluoride (PMSF), 5 μg/ml aprotinin, and 5 μg/ml leupeptin. For the preparation of clonal β-cell membrane fractions, cells were scraped into ice-cold homogenization buffer (0.25 mol/l sucrose, 1 mmol/l EDTA, 20 mmol/l HEPES, 1 μmol/l PMSF, 5 μg/ml aprotinin, and 5 μg/ml leupeptin, pH 7.4) and then homogenized with a Teflon homogenizer on ice. Fractions were collected by differential centrifugation at 4°C as follows: 200*g* for 10 min, whole cell/nuclear fraction; 3,000*g* for 10 min, heavy mitochondrial fraction; 16,000*g* for 10 min, light mitochondrial fraction; 100,000*g* for 1 h, microsomal fraction; and supernatant from 100,000*g* spin, cytosolic fraction.

Generation and purification of polyclonal anti-PMR1 antibody. Rabbit polyclonal antiserum was raised to a 17–amino acid peptide [(C)RRAFHGW NEFDISEDE$_{amide}$] corresponding to a 100% homologous amino-terminal region of rat and human PMR1/ATP2C1 (16,31). Rabbits (New Zealand white) were immunized with keyhole limpet hemocyanin–conjugated peptide, as previously described (32), and the specificity was confirmed by immunoblot analysis (see below). For antibody purification, non-IgG proteins were precipitated from the antiserum with caprylic acid (33), and the IgG fraction was precipitated using ammonium sulfate.

Immunoblotting (Western). Protein samples were resolved by SDS-PAGE on 5–7.5% (wt/vol) polyacrylamide gels and transferred onto Immobilon-P transfer membrane (Millipore) following a standard protocol. Membranes were probed with primary antibodies, as stated in the figure legends. Immunostaining was revealed with horseradish peroxidase (HRP)-conjugated secondary antibodies using an enhanced chemiluminescence detection system (Roche Diagnostics).

Silencing of PMR1 expression using small interfering RNAs. A small interfering RNA (siRNA) duplex corresponding to nucleotides 337–357 of rat PMR1 cDNA (31) was generated (Dharmacon Research). This region showed no significant homology to any other known gene (analyzed using BLAST) (34). The siRNA duplex consisted of a 21-nucleotide sense strand (5′-GUUAGUCAUAGGCGAGCCUdTdT-3′) and a 21-nucleotide antisense strand (5′-AGGCUCGCCUAUGACUAACdTdT-3′), paired in a manner to have a 19-nucleotide duplex region with a 2-nucleotide dithymidine overhang at each 3′ terminus. A scrambled siRNA (sense strand, 5′-CGUGAUUGCGAGACUCUGAdTdT-3′; antisense strand, 5′-UCAGAGUCUCGCAAUCACGdTdT-3′), which showed no significant homology to any protein known (analyzed using BLAST), was used as a control.

siRNAs were introduced into INS1 or MIN6 cells by lipid-mediated transfection using Oligofectamine (Invitrogen). For each 2-cm^2 culture dish, lipid-siRNA complexes were formed using 60 pmol siRNA and 3 μl Oligofectamine in 100 μl Optimem1 serum-free medium (Invitrogen). Lipid complexes were then added to cells that were previously seeded in 400 μl antibiotic-free growth medium. After 24 h, the medium was supplemented with 500 μl growth medium. To measure secretory vesicle, ER, or cytosolic Ca^{2+} concentrations in cells transfected with control (scrambled) or PMR1 siRNAs, cells were infected with VAMP.Aq-, ER.Aq-, or Cyt.Aq-encoding adenovirus 24 h after siRNA transfection. Ca^{2+} measurements were carried out 24 h after adenoviral infection.

Measurements of free [Ca^{2+}] with recombinant targeted aequorins. Where indicated, cells were depleted of Ca^{2+} by incubation with ionomycin (10 μmol/l), monensin (10 μmol/l), and cyclopiazonic acid (10 μmol/l) in modified Krebs-Ringer bicarbonate buffer (KRBB, 140 mmol/l NaCl, 3.5 mmol/l KCl, 0.5 mmol/l NaH_2PO_4, 0.5 mmol/l $MgSO_4$, 3 mmol/l glucose, 10 mmol/l HEPES, and 2 mmol/l $NaHCO_3$, pH 7.4), supplemented with 1 mmol/l EGTA, for 10 min at 4°C (7). Aequorin was reconstituted with 5 μmol/l coelenterazine (Cyt.Aq) or 5 μmol/l coelenterazine *n* (VAMP.Aq and ER.Aq) for 1–2 h at 4°C in KRBB supplemented with 1 mmol/l EGTA.

Intact cells were perifused with KRBB supplemented with additions as stated, at a flow rate of 2 ml/min in a thermostatted chamber (37°C) in close proximity to a photomultiplier tube (ThornEMI) (35). Where indicated, cells were permeabilized with 20 μmol/l digitonin (Fluka) for 1 min at 37°C and subsequently perifused in intracellular buffer (140 mmol/l KCl, 10 mmol/l NaCl, 1 mmol/l KH_2PO_4, 5.5 mmol/l glucose, 2 mmol/l $MgSO_4$, 1 mmol/l ATP, 2 mmol/l sodium succinate, and 20 mmol/l HEPES, pH 7.05), with additions as stated in the figure legends. At the end of all experiments, cells were lysed in a hypotonic Ca^{2+}-rich solution (100 μmol/l digitonin and 10 mmol/l Ca^{2+} in H_2O) to discharge the remaining aequorin pool for calibration of the aequorin signal (7).

Imaging [Ca^{2+}] oscillations in single cells. MIN6 cells were incubated for 16 h in full growth medium containing 3 mmol/l glucose. Cells were then loaded with 5 μmol/l fluo-3-acetoxymethylester (fluo-3-AM; Sigma) for 40 min at 37°C in KRBB containing 3 mmol/l glucose. $[Ca^{2+}]_{cyt}$ changes in individual cells were imaged after stimulation, as stated in the figure legends, using an Olympus IX-70 inverted microscope (×40 objective lens). Cells were excited at 480 nm at 5-s intervals using a Till photonics monochromator, and emission signals were detected at 515 nm with an Imago SensiCam cooled charge-coupled device camera.

Assay of insulin secretion. MIN6 cells were incubated in full growth medium containing 3 mmol/l glucose for 16 h and then incubated in KRBB supplemented with 3 mmol/l glucose for 15 min at 37°C. The medium was removed, and then the cells were stimulated for a further 40 min at 37°C with KRBB plus additions, as stated in the figure legends. Released and total insulin were measured by radioimmunoassay (36).

Statistics. Free [Ca^{2+}] was calculated using the METLIG program (37). Data represent the means ± SE of at least three separate experiments. Statistical analysis was performed using Student's *t* test.

RESULTS

Expression of PMR1 in rat islets and clonal β-cells. To determine whether PMR1 mRNA is present in primary rat islets or clonal β-cells, PCR amplification was performed using primers designed to amplify a 640-bp internal region of rat PMR1 cDNA (31). A fragment of the correct size was amplified from islet, INS1-derived (rat), and MIN6-derived (mouse) cDNA (Fig. 1*A*). The mRNA encoding mouse PMR1 was subsequently cloned from MIN6 cells (see online appendix [available at http://diabetes.diabetesjournals.org]). In extracts from either rat islets or

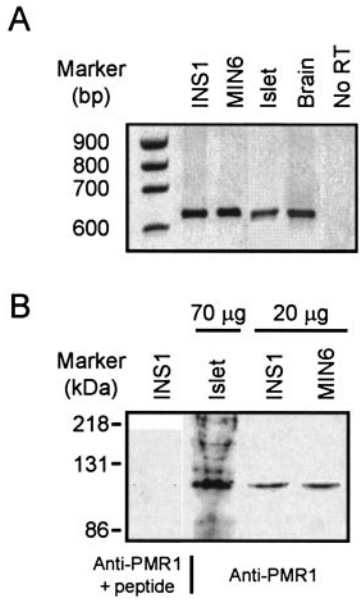

FIG. 1. Expression of PMR1 in primary rat islets and clonal β-cell lines. *A*: Total RNA was extracted from INS1 and MIN6 cells, rat islets, and rat brain; reverse-transcribed; and amplified using PCR with primers designed to amplify a 640-bp internal region of PMR1. A negative control (No RT) was performed using non–reverse-transcribed RNA as a template for PCR. The sequence of the mouse clone is given in the online appendix (Gene Bank accession no. AJ551270). *B*: Rat islet protein (70 µg per lane) or whole-cell lysate from INS1 or MIN6 cells (20 µg per lane) was separated on a 7.5% (wt/vol) polyacrylamide gel, blotted onto Immobilon-P transfer membrane, and probed with anti-PMR1 antibody (1:1,000) in the absence or presence (as indicated, at 40 µg/ml) of the 17–amino acid peptide used for antibody generation. HRP-conjugated anti-rabbit IgG secondary antibody (1:80,000; Sigma) was used for visualization.

clonal β-cells, the presence of the 105-kDa PMR1 protein was revealed by immunoblotting with a polyclonal antibody raised to the amino terminus of PMR1 (Fig. 1*B*). Furthermore, immunoblotting of subcellular fractions separated by differential centrifugation revealed a widespread distribution of PMR1 on both INS1 (Fig. 2*A*) and MIN6 (Fig. 2*B*) cell membranes. As predicted, PMR1 immunoreactivity was enriched in microsomal fractions, identified by the presence of the type II ryanodine receptor (RyR II) (Fig. 2*A*) (8). In addition, a substantial proportion of PMR1 immunoreactivity from either cell type was detected in a heavy mitochondrial fraction that was also rich in dense-core secretory vesicles (see measurements of insulin content in Fig. 2*A*). However, suggesting that PMR1 was largely confined to ER-, Golgi-, and dense-core vesicle–associated membranes, we were unable to detect any labeling of plasma membrane or mitochondrial structures by immunocytochemical analysis of overexpressed c-*myc*-PMR1, but there was substantial overlap with markers for the secretory pathway (results not shown).

Silencing of PMR1 protein using siRNA. To investigate the role(s) of PMR1 in β-cells, endogenous PMR1 protein expression was reduced by RNA silencing, and the effect on intracellular Ca^{2+} handling was monitored using recombinant targeted aequorins (38). Transfection of an siRNA duplex corresponding to nucleotides 337–357 of rat PMR1 cDNA (PMR1 siRNA) (31) reduced PMR1 expression in INS1 cells by 65.3 ± 11.9 and 85.7 ± 4.7% ($n = 3$, $P < 0.01$) after 24 and 48 h, respectively, consistent with the efficient transfection of the duplex RNA into at least 85% of the cell population. PMR1 levels remained low until 72 h after transfection, when expression increased to 70.3 ± 4.4% ($n = 3$, $P < 0.01$) of the control level (Fig. 3*A*). After PMR1 siRNA transfection, a similar reduction in PMR1 expression was observed in MIN6 cells, indicating that the chosen siRNA was also effective for depleting mouse PMR1 mRNA (Fig. 3*A*). This silencing effect appeared to be selective because PMR1 siRNA transfection of INS1 cells did not affect SERCA2 or mannose 6-phosphate receptor (m6PR) protein expression (Fig. 3*B*). Conversely, PMR1 expression was unaffected after transfection with a control (scrambled) siRNA (Fig. 3*A*).

Effect of PMR1 silencing on Ca^{2+} influx and intracellular Ca^{2+} homeostasis. Previous studies in both yeast (19) and mammalian cells (20) have revealed a role for PMR1 in controlling Ca^{2+} influx. We explored the effect of PMR1 silencing on Ca^{2+} influx in intact INS1 β-cells by monitoring changes in $[Ca^{2+}]_{cyt}$ when Ca^{2+} was reintroduced to Ca^{2+}-depleted cells, a condition in which store-operated Ca^{2+} channels are activated (7). The rate of increase of $[Ca^{2+}]_{cyt}$ and the initial $[Ca^{2+}]_{cyt}$ peak were markedly increased in cells treated with PMR1 siRNA (Fig. 4*A*, Table 1), and $[Ca^{2+}]_{cyt}$ remained significantly higher in PMR1-depleted cells for ~1 min before returning to control levels.

In yeast *pmr1*-null mutants, one of the essential compo-

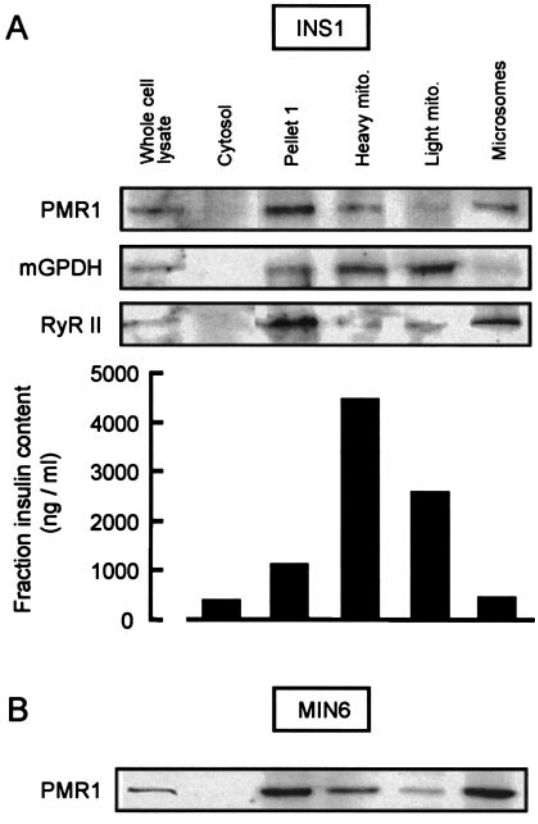

FIG. 2. Immunoblot of clonal β-cell fractions separated by differential centrifugation. INS1 (*A*) or MIN6 (*B*) cell fractions (20 µg per lane) were probed with rabbit anti-PMR1 (1:1,000) or, in *A*, with rabbit anti–mitochondrial glycerol phosphate dehydrogenase (mGPDH; 1:500; mitochondrial marker) or mouse anti–RyR II (1:1,000; ER marker). Immunoreactivity was visualized with anti-rabbit IgG HRP (1:80,000; Sigma) or anti-mouse IgG HRP (1:10,000; Sigma). INS1 fraction insulin content was measured by radioimmunoassay. Results shown are representative of three separate experiments performed for each cell type.

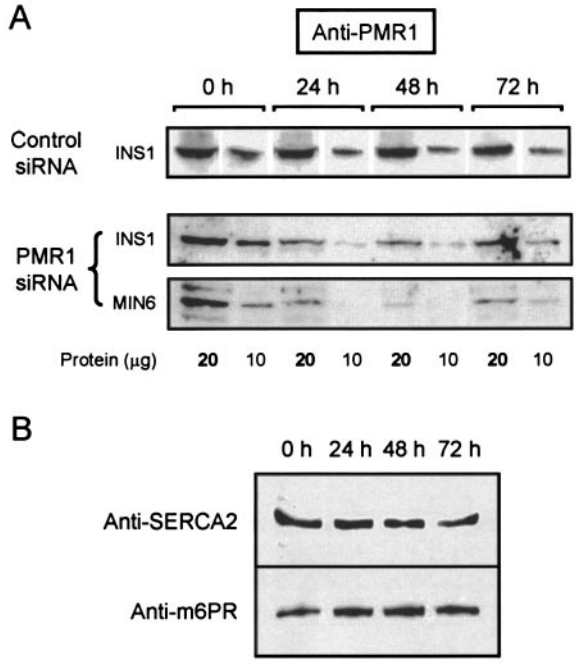

FIG. 3. Silencing of endogenous PMR1 using siRNA. *A*: INS1 or MIN6 whole-cell lysates were prepared 0, 24, 48, and 72 h after transfection with control scrambled siRNA or PMR1 siRNA (as indicated). For each lane, 20 μg protein (or 10 μg where indicated) of siRNA-treated cell lysates were probed with rabbit anti-PMR1 (1:1,000) or, in *B*, with goat anti-SERCA2 (1:500; Santa Cruz) or rabbit anti-m6PR (1:1,000; Affinity BioReagents). Immunoreactivity was visualized with anti-rabbit IgG HRP (1:80,000; Sigma) or anti-goat HRP (1:10,000; Sigma). Each image is representative of three separate experiments for each cell type.

nents of the high-affinity Ca^{2+} influx system stimulated by store depletion has been identified as a homologue of the α1 pore-forming subunit of voltage-gated Ca^{2+} channels (19). To determine whether voltage-gated Ca^{2+} channels might be involved in the elevation of $[Ca^{2+}]_{cyt}$ observed in PMR1-depleted β-cells, $CaCl_2$ was reintroduced to Ca^{2+}-depleted cells in the presence of the voltage-gated Ca^{2+} channel inhibitor nimodipine. Under these conditions, the elevation of $[Ca^{2+}]_{cyt}$ previously observed in PMR1-depleted cells was completely abolished, and the peak value achieved (~1.7 μmol/l) was identical in cells treated with either scrambled or PMR1 siRNAs (Fig. 4*B*, Table 1). Interestingly, in the presence of nimodipine, the initial $[Ca^{2+}]$ peak was not followed by an elevated $[Ca^{2+}]$ plateau that is normally observed in the absence of the drug (Fig. 4*A* versus 4*B*), indicating that this sustained elevation of $[Ca^{2+}]_{cyt}$ is dependent on Ca^{2+} influx through L-type Ca^{2+} channels.

These results indicated that Ca^{2+} entry via voltage-gated Ca^{2+} channels was largely responsible for the enhancement of Ca^{2+} entry in PMR1-depleted β-cells. To determine whether the enhanced increases in $[Ca^{2+}]_{cyt}$ after Ca^{2+} readmission to PMR1-depleted cells may be attributable to alterations in the expression or activity of voltage-gated Ca^{2+} channels or to other factors such as alterations in membrane potential, we monitored increases in $[Ca^{2+}]_{cyt}$ provoked by cell depolarization with 50 mmol/l KCl. Neither the peak nor sustained $[Ca^{2+}]_{cyt}$ values were affected by PMR1 depletion (Fig. 4*C*), arguing against a role for changes in the activity or total number of voltage-gated Ca^{2+} channels. Correspondingly, PMR1 depletion had no effect on levels of mRNA encoding the L-type Ca^{2+} channel α1 subunit (data not shown).

After the initial peak of $[Ca^{2+}]_{cyt}$ after the reintroduction of $CaCl_2$ to control or PMR1 siRNA–treated cells, $[Ca^{2+}]_{cyt}$ returned to basal levels after ~1 min, a process likely to involve extrusion of Ca^{2+} across the plasma membrane and pumping of the ion into intracellular stores. To examine the effect this Ca^{2+} accumulation may have on organelle lumen Ca^{2+} concentrations, we monitored changes in secretory vesicle and ER Ca^{2+} concentration in intact cells. The rate and extent of ER Ca^{2+} uptake were markedly increased (Fig. 4*E*, Table 1) after PMR1 silencing, presumably reflecting the increase in $[Ca^{2+}]_{cyt}$ observed under these conditions (Fig. 4*A*), whereas vesicular $[Ca^{2+}]$ was unaffected (Fig. 4*D*, Table 1). Accordingly, the augmented ER $[Ca^{2+}]$ observed in PMR1-depleted cells was completely abolished by the presence of nimodipine (Fig. 4*F*, Table 1).

Role of PMR1 in organellar Ca^{2+} uptake. Because the above measurements in intact cells were complicated by changes in $[Ca^{2+}]_{cyt}$ after PMR1 depletion, we next explored changes in organellar $[Ca^{2+}]$ using digitonin-permeabilized cells in which $[Ca^{2+}]_{cyt}$ could be clamped at will. When perifusate $[Ca^{2+}]$ was increased from <1 to 400 nmol/l, the initial rate of $[Ca^{2+}]$ increase in both the secretory vesicles (3.36 ± 0.42 vs. 2.33 ± 0.14 $\mu mol \cdot l^{-1} \cdot s^{-1}$ for control vs. $PMR1^-$ cells, $n = 3$, $P < 0.05$) (Fig. 4*G*) and the ER (3.62 ± 0.48 vs. 2.00 ± 0.28 $\mu mol \cdot l^{-1} \cdot s^{-1}$, $n = 3$, $P < 0.01$) (Fig. 4*H*) was found to be significantly inhibited in PMR1-depleted compared with control cells, whereas steady-state Ca^{2+} concentrations were not significantly different in the two groups.

Effect of PMR1 silencing on insulin secretion and $[Ca^{2+}]$ oscillations. We next investigated the effect of PMR1 silencing on insulin secretion stimulated by glucose. MIN6 cells were used for these experiments because of their greater responsiveness to nutrient secretagogues compared with INS1 cells (39). The stimulation of insulin secretion in response to 30.0 mmol/l (vs. 3.0 mmol/l) glucose was significantly increased by PMR1 depletion (4.3 ± 0.8 vs. 6.3 ± 0.8-fold stimulation for control vs. $PMR1^-$ cells, $n = 4$, $P < 0.05$) (Fig. 5*A*). In contrast, basal insulin secretion (3.0 mmol/l glucose) or secretion stimulated by a submaximal glucose concentration (11.0 mmol/l) were unaffected by PMR1 silencing (Fig. 5*A*).

From the data shown in Fig. 4, we inferred that the enhancement of glucose-induced insulin secretion observed in PMR1-depleted cells may be attributable to increased Ca^{2+} influx. However, measurements with Cyt.Aq revealed that after stimulation with 30.0 mmol/l glucose, average $[Ca^{2+}]_{cyt}$ was unaffected by PMR1 silencing (data not shown). Therefore, we explored the possibility that PMR1 depletion enhances glucose-induced insulin secretion by modifying spatial or temporal aspects of the evoked $[Ca^{2+}]$ increases. In the additional presence of tetraethylammonium (TEA), an inhibitor of Ca^{2+}- and voltage-activated K^+ channels (40) that amplifies glucose-induced $[Ca^{2+}]$ oscillations in single MIN6 cells (39), there was no significant difference in the average $[Ca^{2+}]_{cyt}$ between control and PMR1-depleted cells: 43.81 ± 6.37 vs.

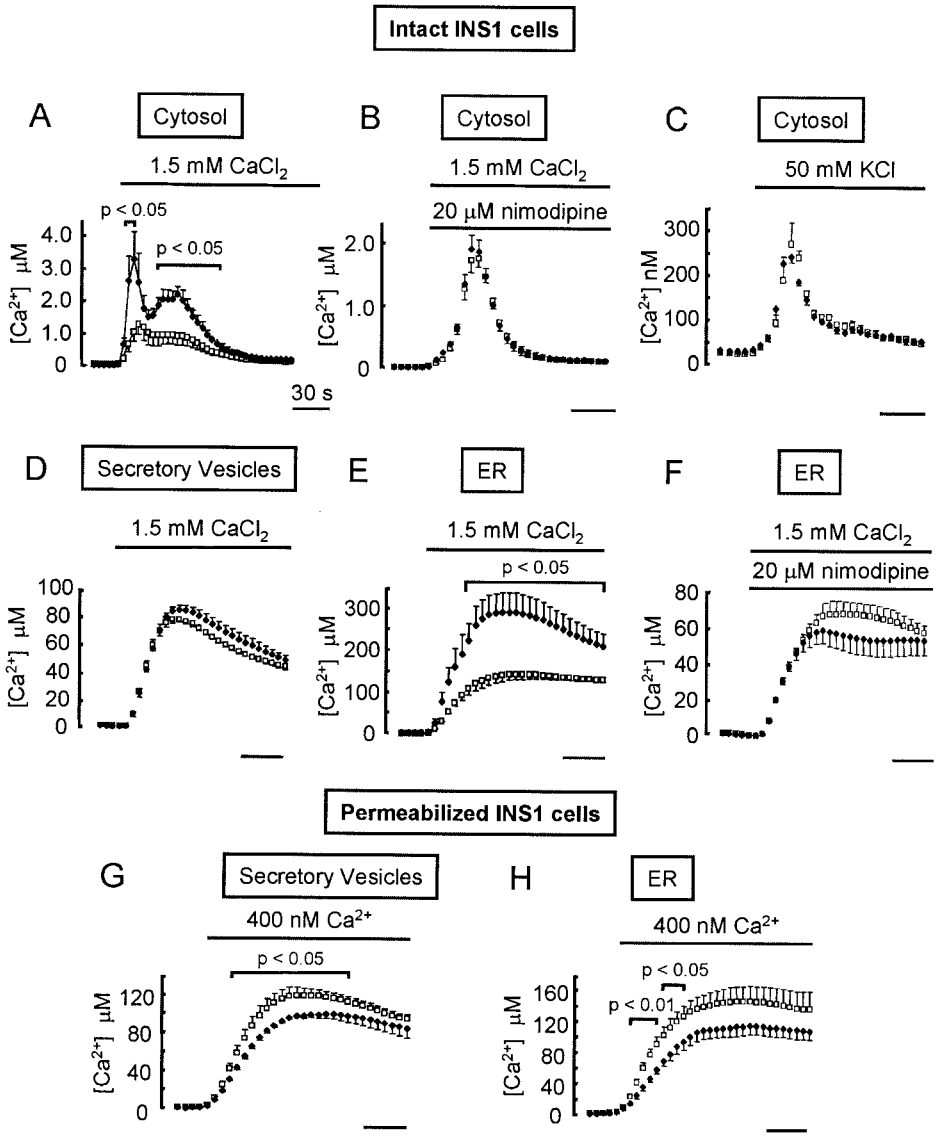

FIG. 4. Measurements of organelle free Ca^{2+} in PMR1-depleted cells. PMR1 siRNA-transfected (♦) or control scrambled siRNA-transfected (□) INS1 cells were infected with Cyt.Aq-encoding (*A–C*), VAMP.Aq-encoding (*D* and *G*), or ER.Aq-encoding (*E*, *F*, and *H*) adenoviruses 24 h after siRNA transfection. *A*, *B*, and *D–H*: After a further 24 h, cells were depleted of Ca^{2+}, the aequorin reconstituted in Ca^{2+}-free KRBB, and then cells were perifused with KRBB supplemented with 1 mmol/l EGTA. In intact cells, 1 mmol/l EGTA was replaced with 1.5 mmol/l $CaCl_2$ where indicated. *G* and *H*: Cells were permeabilized with 20 μmol/l digitonin in intracellular buffer containing 1 mmol/l EGTA (free $[Ca^{2+}]$ <1 nmol/l) and then, where indicated, free $[Ca^{2+}]$ was increased to 400 nmol/l using an EGTA-buffered Ca^{2+} solution. *C*: At 24 h after adenoviral infection, cells were reconstituted with coelenterazine in KRBB containing 1.5 mmol/l $CaCl_2$. Cells were perifused in the same medium before stimulation with 50 mmol/l KCl. In all experiments, cells were finally lysed in hypotonic medium containing 100 μmol/l digitonin and 10 mmol/l $CaCl_2$. In all cases, data are the means of four separate experiments.

50.19 ± 6.72% change for control vs. $PMR1^-$ cells, $n = 10$ cells (Fig. 5*C*), corresponding to a $[Ca^{2+}]_{cyt}$ of ~330 nmol/l (basal values ~200 nmol/l), as measured in single cells using fluo-3-AM and in cell populations using Cyt.Aq (data not shown). In contrast, PMR1 depletion appeared to transform the $[Ca^{2+}]$ changes into slow oscillations, with rapid oscillations superimposed at the peak but not at the nadir (Fig. 5*B*). The amplitude of these slow oscillations was not affected by PMR1 silencing (126.8 ± 9.8 vs. 133.23 ± 9.1% change for control vs. $PMR1^-$ cells, $n = 10$ cells) (Fig. 5*D*). However, oscillation duration (29.61 ± 1.4 vs. 71.28 ± 10.7 s for control vs. $PMR1^-$ cells, $n = 10$ cells, $P < 0.001$) (Fig. 5*E*) and decay rate on return to nadir (4.33 ± 0.27 vs. 7.17 ± 1.01 s, control vs. $PMR1^-$ cells, $n = 10$ cells, $P < 0.05$) (Fig. 5*F*) were significantly increased. Correspondingly, insulin secretion was significantly enhanced in PMR1-depleted cells when stimulated under the same conditions (11 mmol/l glucose + 10 mmol/l TEA; 5.9 ± 1.5 vs. 10.9 ± 2.5-fold stimulation for control vs. $PMR1^-$ cells, $n = 4$, $P < 0.05$) (Fig. 5*A*).

TABLE 1
Effects of PMR1 silencing on Ca^{2+} uptake and intracellular steady-state Ca^{2+} concentrations in intact cells

Compartment	Initial rate of $[Ca^{2+}]$ rise ($\mu mol \cdot l^{-1} \cdot s^{-1}$)		Peak $[Ca^{2+}]$ (μmol/l)	
	Control	$PMR1^-$	Control	$PMR1^-$
Cytosol	0.07 ± 0.03	0.44 ± 0.18*	1.25 ± 0.31	3.24 ± 1.00†
Cytosol + nimodipine	0.07 ± 0.01	0.07 ± 0.01	1.65 ± 0.13	1.80 ± 0.22
Secretory vesicles	3.49 ± 0.53	3.41 ± 0.53	120.88 ± 2.12	125.40 ± 16.56
ER	3.57 ± 0.26	12.20 ± 2.12†	142.99 ± 12.79	291.30 ± 45.23†
ER + nimodipine	2.19 ± 0.25	2.23 ± 0.19	68.41 ± 6.55	56.61 ± 8.70

Control and $PMR1^-$ indicate data for cells treated with scrambled or PMR1 siRNAs, respectively. *Significance where $P < 0.05$; †$P < 0.01$.

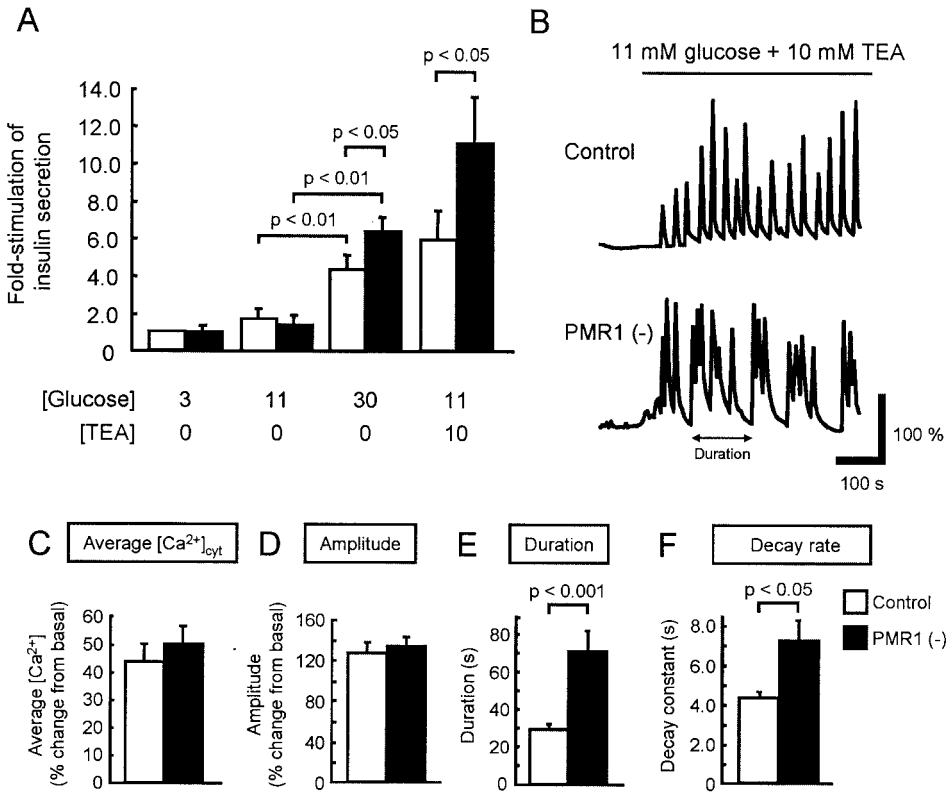

FIG. 5. Effect of PMR1 silencing on glucose-stimulated insulin secretion. *A*: MIN6 cells were cultured for 16 h at 3 mmol/l glucose and then incubated with KRBB supplemented with 3 mmol/l glucose for 15 min. Cells were then incubated for a further 40 min in KRBB supplemented with 3, 11, or 30 mmol/l glucose, or with 11 mmol/l glucose plus 10 mmol/l TEA. Released and total insulin were measured by radioimmunoassay. Data are the means of at least three separate experiments. Basal insulin secretion (at 3 mmol/l glucose) was not significantly different in control and PMR1-depleted cells (0.12 and 0.11% of total insulin per 40 min, respectively; means of two separate experiments). *B*: After culturing for 16 h at 3 mmol/l glucose, MIN6 cells were loaded with fluo-3-AM for 40 min in KRBB containing 3 mmol/l glucose. Cells were then challenged with KRBB supplemented with 11 mmol/l glucose plus 10 mmol/l TEA. Ca^{2+} oscillations were monitored on a Olympus IX-70 inverted microscope (excitation 480 nm, emission 515 nm). *C*: Average $[Ca^{2+}]_{cyt}$ calculated by integrating $[Ca^{2+}]$ over the final 5 min of stimulation with 11 mmol/l glucose and 10 mmol/l TEA for control and PMR1 siRNA–treated cells. *D–F*: Amplitude (*D*), duration (measured as indicated in *B*) (*E*), and decay rate (*F*) of slow $[Ca^{2+}]_{cyt}$ oscillations during the final 5 min of stimulation with 11 mmol/l glucose and 10 mmol/l TEA for control and PMR1 siRNA–treated cells. *C–F*: Data are the means of at least 10 cells in each case. □, control; ■, $PMR1^{-}$.

DISCUSSION

PMR1 is present on multiple intracellular membranes in islet β-cells. We show here that PMR1/ATP2C1 is expressed in both pancreatic islets and clonal β-cells derived from both rat and mouse (Fig. 1). In contrast to previous studies that have shown a predominantly Golgi localization of endogenous PMR1 in yeast (14) and overexpressed PMR1 in mammalian cell lines (20,41), the present study reveals the presence of endogenous PMR1 in two distinct fractions containing either ER (RyR II) or secretory vesicle (insulin) markers (Fig. 2). In agreement with this distribution, we demonstrate that inactivation of the pump with selective siRNAs has marked effects on Ca^{2+} handling by both the ER and secretory vesicles in these cells. Importantly, these findings demonstrate that PMR1 plays a significant role in the accumulation of Ca^{2+} by the ER (Fig. 4*H*) and may underlie the thapsigargin-independent uptake of Ca^{2+} into this compartment (7,42, 43), which represents 15–20% of the total Ca^{2+} uptake capacity of this organelle. We also show here that PMR1 contributes ~20% to the Ca^{2+} uptake capacity of dense-core secretory vesicles in β-cells (Fig. 4*G*), although the identity of the remaining Ca^{2+}-ATPase activity (7) remains to be established. However, the limited effect of PMR1 depletion on organelle Ca^{2+} sequestration appears to be too small to impact on $[Ca^{2+}]_{cyt}$ in intact cells (Fig. 4*B–C*), where alternative mechanisms, including the plasma membrane Ca^{2+}-ATPase and Na^{+}/Ca^{2+} exchange, act in concert with Ca^{2+} sequestration via SERCA pumps to clear Ca^{2+} from the cytosol (44). Indeed, PMR1 depletion did not significantly affect organelle steady-state $[Ca^{2+}]$ (Fig. 4*G–H*), consistent with a relatively minor role for this pump in overall Ca^{2+} clearance.

PMR1 depletion enhances Ca^{2+} influx through voltage-gated Ca^{2+} channels. PMR1 silencing in β-cells had a dramatic effect on the increases in $[Ca^{2+}]_{cyt}$ observed after the reintroduction of $CaCl_2$ to previously Ca^{2+}-depleted cells, and this is likely to be caused, at least in part, by an activation of Ca^{2+} influx. Correspondingly, the enhanced $[Ca^{2+}]$ increases observed in PMR1-depleted cells were eliminated by the blockade of L-type Ca^{2+} channels with nimodipine. These observations are reminiscent of the effect of *pmr1* deletion in *S. cerevisiae* (19). Previous findings in islets have suggested that depletion of thapsigargin-sensitive Ca^{2+} stores potentiates voltage-dependent Ca^{2+} influx, in part by stimulating a depolarizing current carried by store-operated Ca^{2+} channels (45). In addition, K^{+}-induced Ca^{2+} influx was stimulated in $SERCA3^{-/-}$ mouse islets (46). By contrast, in the present study we found that PMR1 depletion had no effect on K^{+}-induced $[Ca^{2+}]_{cyt}$ increases, suggesting that indirect mechanisms, possibly involving changes in plasma membrane potential, are responsible for the effects of PMR1 depletion on Ca^{2+} influx via voltage-gated Ca^{2+} channels. In contrast to the effects of thapsigargin (45), it seems unlikely that increased Ca^{2+} influx via store-operated Ca^{2+} channels underlies the plasma membrane depolarization in the absence of PMR1. Thus, no differences were observed between control and PMR1-deficient cells in terms of the $[Ca^{2+}]_{cyt}$ increases provoked by the readdition of $CaCl_2$ in the presence of nimodipine (Fig. 4*B*). Instead, activation of a store-dependent current, possibly the depolarizing nonselective cation current primarily carried by Na^{+} that was previously described by Dukes and colleagues (47–49), might explain the enhanced influx of Ca^{2+} through voltage-gated channels after depletion of

PMR1. Detailed electrophysiological studies will be required both to characterize the effect(s) of PMR1 ablation on these and other polarizing or depolarizing currents and to explore in detail the mechanisms by which depletion of a PMR1-dependent Ca^{2+} store may affect these currents.

PMR1 depletion enhances glucose-induced insulin secretion. Suppression of PMR1 caused a significant enhancement of glucose-stimulated, but not basal, insulin secretion (Fig. 5*A*). This result is similar to the effects of thapsigargin, which augments glucose-induced, but not basal, insulin secretion from isolated islets (50). The effects of PMR1 suppression seen here were not associated with an increase in average $[Ca^{2+}]_{cyt}$ but a modification of $[Ca^{2+}]$ oscillation shape. Thus, PMR1 depletion transformed rapid transients into broader $[Ca^{2+}]$ increases, on which rapid nonbaseline increases were superimposed (Fig. 5*B*). The fact that $[Ca^{2+}]_{cyt}$ remains elevated for longer periods in PMR1-depleted cells during the slow oscillations may underlie the enhanced secretion, although other mechanisms may also be involved. Importantly, if the principal role of PMR1 were to mediate Ca^{2+} sequestration from the cytosol, then after PMR1 depletion one would expect to observe an increase in oscillation amplitude caused by decreased Ca^{2+} buffering, a response similar to that observed in SERCA3$^{-/-}$ mouse islets (46). In contrast, PMR1 depletion had no effect on oscillation amplitude, but instead it prolonged oscillation duration, supporting our proposal (see above) that the primary role of PMR1 is not to sequester cytosolic Ca^{2+} per se. Instead, the most important roles of this Ca^{2+}-ATPase appear to contribute to Ca^{2+} uptake by secretory vesicles and to modulate, albeit by an indirect mechanism, the activity of plasma membrane L-type Ca^{2+} channels.

ACKNOWLEDGMENTS

This study was supported by a Biotechnology and Biological Sciences Research Council Studentship (to K.J.M.) and grants to G.A.R from the Wellcome Trust (Program Grant 067081/Z/02/Z), the Human Frontiers Science Program, the Medical Research Council (U.K.), and Diabetes U.K. G.A.R. is a Wellcome Trust Research Leave Fellow.

We thank Rebecca Rowe for the preparation of pancreatic islets and Professor Anant Parekh (University of Oxford) for useful discussion.

REFERENCES

1. Bryan J, Aguilar-Bryan L: The ABCs of ATP-sensitive potassium channels: more pieces of the puzzle. *Curr Opin Cell Biol* 9:553–559, 1997
2. Safayhi H, Haase H, Kramer U, Bihlmayer A, Roenfeldt M, Ammon HP, Froschmayr M, Cassidy TN, Morano I, Ahlijanian MK, Striessnig J: L-type calcium channels in insulin-secreting cells: biochemical characterization and phosphorylation in RINm5F cells. *Mol Endocrinol* 11:619–629, 1997
3. Gilon P, Arredouani A, Gailly P, Gromada J, Henquin JC: Uptake and release of Ca^{2+} by the endoplasmic reticulum contribute to the oscillations of the cytosolic Ca^{2+} concentration triggered by Ca^{2+} influx in the electrically excitable pancreatic B-cell. *J Biol Chem* 274:20197–20205, 1999
4. Wollheim CB, Biden TJ: Second messenger function of inositol 1, 4, 5-trisphosphate: early changes in inositol phosphates, cytosolic Ca^{2+}, and insulin release in carbamylcholine-stimulated RINm5F cells. *J Biol Chem* 261:8314–8319, 1986
5. Rutter GA: Nutrient-secretion coupling in the pancreatic islet beta-cell: recent advances. *Mol Aspects Med* 22:247–284, 2001
6. Tengholm A, Hellman B, Gylfe E: The endoplasmic reticulum is a glucose-modulated high-affinity sink for Ca^{2+} in mouse pancreatic beta-cells. *J Physiol* 530:533–540, 2001
7. Mitchell KJ, Pinton P, Varadi A, Tacchetti C, Ainscow EK, Pozzan T, Rizzuto R, Rutter GA: Dense core secretory vesicles revealed as a dynamic Ca(2+) store in neuroendocrine cells with a vesicle-associated membrane protein aequorin chimaera. *J Cell Biol* 155:41–51, 2001
8. Mitchell KJ, Lai FA, Rutter GA: Ryanodine receptor type I and nicotinic acid adenine dinucleotide phosphate (NAADP) receptors mediate Ca^{2+} release from insulin-containing vesicles in living pancreatic beta-cells (MIN6). *J Biol Chem* 278:11057–11067, 2003
9. Emmanouilidou E, Teschemacher AG, Pouli AE, Nicholls LI, Seward EP, Rutter GA: Imaging Ca^{2+} concentration changes at the secretory vesicle surface with a recombinant targeted cameleon. *Curr Biol* 9:915–918, 1999
10. Shull GE: Gene knockout studies of Ca^{2+}-transporting ATPases. *Eur J Biochem* 267:5284–5290, 2000
11. Rudolph HK, Antebi A, Fink GR, Buckley CM, Dorman TE, LeVitre J, Davidow LS, Mao JI, Moir DT: The yeast secretory pathway is perturbed by mutations in PMR1, a member of a Ca^{2+} ATPase family. *Cell* 58:133–145, 1989
12. Wuytack F, Raeymaekers L, Missiaen L: Molecular physiology of the SERCA and SPCA pumps. *Cell Calcium* 32:279–305, 2002
13. Sorin A, Rosas G, Rao R: PMR1, a Ca^{2+}-ATPase in yeast Golgi, has properties distinct from sarco/endoplasmic reticulum and plasma membrane calcium pumps. *J Biol Chem* 272:9895–9901, 1997
14. Antebi A, Fink GR: The yeast Ca(2+)-ATPase homologue, PMR1, is required for normal Golgi function and localizes in a novel Golgi-like distribution. *Mol Biol Cell* 3:633–654, 1992
15. Missiaen L, Van Acker K, Parys JB, De Smedt H, Van Baelen K, Weidema AF, Vanoevelen J, Raeymaekers L, Renders J, Callewaert G, Rizzuto R, Wuytack F: Baseline cytosolic Ca^{2+} oscillations derived from a non-endoplasmic reticulum Ca^{2+} store. *J Biol Chem* 276:39161–39170, 2001
16. Hu Z, Bonifas JM, Beech J, Bench G, Shigihara T, Ogawa H, Ikeda S, Mauro T, Epstein EH Jr: Mutations in ATP2C1, encoding a calcium pump, cause Hailey-Hailey disease. *Nat Genet* 24:61–65, 2000
17. Sudbrak R, Brown J, Dobson-Stone C, Carter S, Ramser J, White J, Healy E, Dissanayake M, Larregue M, Perrussel M, Lehrach H, Munro CS, Strachan T, Burge S, Hovnanian A, Monaco AP: Hailey-Hailey disease is caused by mutations in ATP2C1 encoding a novel Ca(2+) pump. *Hum Mol Genet* 9:1131–1140, 2000
18. Halachmi D, Eilam Y: Elevated cytosolic free Ca^{2+} concentrations and massive Ca^{2+} accumulation within vacuoles, in yeast mutant lacking PMR1, a homolog of Ca^{2+}-ATPase. *FEBS Lett* 392:194–200, 1996
19. Locke EG, Bonilla M, Liang L, Takita Y, Cunningham KW: A homolog of voltage-gated Ca(2+) channels stimulated by depletion of secretory Ca(2+) in yeast. *Mol Cell Biol* 20:6686–6694, 2000
20. Missiaen L, Vanoevelen J, Van Acker K, Raeymaekers L, Parys JB, Callewaert G, Wuytack F, De Smedt H: Ca(2+) signals in Pmr1-GFP-expressing COS-1 cells with functional endoplasmic reticulum. *Biochem Biophys Res Commun* 294:249–253, 2002
21. Fraser AG, Kamath RS, Zipperlen P, Martinez-Campos M, Sohrmann M, Ahringer J: Functional genomic analysis of *C. elegans* chromosome I by systematic RNA interference. *Nature* 408:325–330, 2000
22. Hammond SM, Bernstein E, Beach D, Hannon GJ: An RNA-directed nuclease mediates post-transcriptional gene silencing in *Drosophila* cells. *Nature* 404:293–296, 2000
23. Zhao F, Li P, Chen SR, Louis CF, Fruen BR: Dantrolene inhibition of ryanodine receptor Ca^{2+} release channels: molecular mechanism and isoform selectivity. *J Biol Chem* 276:13810–13816, 2001
24. Elbashir SM, Harborth J, Lendeckel W, Yalcin A, Weber K, Tuschl T: Duplexes of 21-nucleotide RNAs mediate RNA interference in cultured mammalian cells. *Nature* 411:494–498, 2001
25. Asfari M, Janjic D, Meda P, Li G, Halban PA, Wollheim CB: Establishment of 2-mercaptoethanol-dependent differentiated insulin-secreting cell lines. *Endocrinology* 130:167–178, 1992
26. Miyazaki J, Araki K, Yamato E, Ikegami H, Asano T, Shibasaki Y, Oka Y, Yamamura K: Establishment of a pancreatic beta cell line that retains glucose-inducible insulin secretion: special reference to expression of glucose transporter isoforms. *Endocrinology* 127:126–132, 1990
27. Brini M, Marsault R, Bastianutto C, Alvarez J, Pozzan T, Rizzuto R: Transfected aequorin in the measurement of cytosolic Ca^{2+} concentration ($[Ca^{2+}]c$): a critical evaluation. *J Biol Chem* 270:9896–9903, 1995
28. Montero M, Brini M, Marsault R, Alvarez J, Sitia R, Pozzan T, Rizzuto R: Monitoring dynamic changes in free Ca^{2+} concentration in the endoplasmic reticulum of intact cells. *EMBO J* 14:5467–5475, 1995
29. Rutter GA, Theler JM, Murgia M, Wollheim CB, Pozzan T, Rizzuto R: Stimulated Ca^{2+} influx raises mitochondrial free Ca^{2+} to supramicromolar levels in a pancreatic beta-cell line: possible role in glucose and agonist-induced insulin secretion. *J Biol Chem* 268:22385–22390, 1993
30. Kennedy HJ, Viollet B, Rafiq I, Kahn A, Rutter GA: Upstream stimulatory

factor-2 (USF2) activity is required for glucose stimulation of L-pyruvate kinase promoter activity in single living islet beta-cells. *J Biol Chem* 272: 20636–20640, 1997
31. Gunteski-Hamblin AM, Clarke DM, Shull GE: Molecular cloning and tissue distribution of alternatively spliced mRNAs encoding possible mammalian homologues of the yeast secretory pathway calcium pump. *Biochemistry* 31:7600–7608, 1992
32. Tunwell RE, Wickenden C, Bertrand BM, Shevchenko VI, Walsh MB, Allen PD, Lai FA: The human cardiac muscle ryanodine receptor-calcium release channel: identification, primary structure and topological analysis. *Biochem J* 318:477–487, 1996
33. McKinney MM, Parkinson A: A simple, non-chromatographic procedure to purify immunoglobulins from serum and ascites fluid. *J Immunol Methods* 96:271–278, 1987
34. Altschul SF, Gish W, Miller W, Myers EW, Lipman DJ: Basic local alignment search tool. *J Mol Biol* 215:403–410, 1990
35. Cobbold PH, Rink TJ: Fluorescence and bioluminescence measurement of cytoplasmic free calcium. *Biochem J* 248:313–328, 1987
36. Ainscow EK, Zhao C, Rutter GA: Acute overexpression of lactate dehydrogenase-A perturbs β-cell mitochondrial metabolism and insulin secretion. *Diabetes* 49:1149–1155, 2000
37. Rutter GA, Denton RM: Regulation of NAD^+-linked isocitrate dehydrogenase and 2-oxoglutarate dehydrogenase by Ca^{2+} ions within toluene-permeabilized rat heart mitochondria: interactions with regulation by adenine nucleotides and NADH/NAD^+ ratios. *Biochem J* 252:181–189, 1988
38. Rutter GA, Fasolato C, Rizzuto R: Calcium and organelles: a two-sided story. *Biochem Biophys Res Commun* 253:549–557, 1998
39. Calabrese A, Zhang M, Serre-Beinier V, Caton D, Mas C, Satin LS, Meda P: Connexin 36 controls synchronization of Ca^{2+} oscillations and insulin secretion in MIN6 cells. *Diabetes* 52:417–424, 2003
40. Su J, Yu H, Lenka N, Hescheler J, Ullrich S: The expression and regulation of depolarization-activated K^+ channels in the insulin-secreting cell line INS-1. *Pflugers Arch* 442:49–56, 2001
41. Ton VK, Mandal D, Vahadji C, Rao R: Functional expression in yeast of the human secretory pathway Ca(2+), Mn(2+)-ATPase defective in Hailey-Hailey disease. *J Biol Chem* 277:6422–6427, 2002
42. Hussain A, Garnett C, Klein MG, Tsai-Wu JJ, Schneider MF, Inesi G: Direct involvement of intracellular Ca^{2+} transport ATPase in the development of thapsigargin resistance by Chinese hamster lung fibroblasts. *J Biol Chem* 270:12140–12146, 1995
43. Yu R, Hinkle PM: Rapid turnover of calcium in the endoplasmic reticulum during signaling: studies with cameleon calcium indicators. *J Biol Chem* 275:23648–23653, 2000
44. Chen L, Koh DS, Hille B: Dynamics of calcium clearance in mouse pancreatic β-cells. *Diabetes* 52:1723–1731, 2003
45. Miura Y, Henquin JC, Gilon P: Emptying of intracellular Ca^{2+} stores stimulates Ca^{2+} entry in mouse pancreatic beta-cells by both direct and indirect mechanisms. *J Physiol* 503:387–398, 1997
46. Arredouani A, Guiot Y, Jonas JC, Liu LH, Nenquin M, Pertusa JA, Rahier J, Rolland JF, Shull GE, Stevens M, Wuytack F, Henquin JC, Gilon P: SERCA3 ablation does not impair insulin secretion but suggests distinct roles of different sarcoendoplasmic reticulum Ca^{2+} pumps for Ca^{2+} homeostasis in pancreatic β-cells. *Diabetes* 51:3245–3253, 2002
47. Worley JF III, McIntyre MS, Spencer B, Mertz RJ, Roe MW, Dukes ID: Endoplasmic reticulum calcium store regulates membrane potential in mouse islet beta-cells. *J Biol Chem* 269:14359–14362, 1994
48. Worley JF III, McIntyre MS, Spencer B, Dukes ID: Depletion of intracellular Ca^{2+} stores activates a maitotoxin-sensitive nonselective cationic current in beta-cells. *J Biol Chem* 269:32055–32058, 1994
49. Roe MW, Worley JF III, Qian F, Tamarina N, Mittal AA, Dralyuk F, Blair NT, Mertz RJ, Philipson LH, Dukes ID: Characterization of a Ca^{2+} release-activated non-selective cation current regulating membrane potential and [Ca^{2+}] oscillations in transgenically derived beta-cells. *J Biol Chem* 273: 10402–10410, 2003
50. Aizawa T, Yada T, Asanuma N, Sato Y, Ishihara F, Hamakawa N, Yaekura K, Hashizume K: Effects of thapsigargin, an intracellular Ca^{2+} pump inhibitor, on insulin release by rat pancreatic B-cell. *Life Sci* 57:1375–1381, 1995